

# Review Article: Hydrogenated graphene: A user's guide <sup>EP</sup>

Cite as: J. Vac. Sci. Technol. A **36**, 05G401 (2018); <https://doi.org/10.1116/1.5034433>

Submitted: 11 April 2018 . Accepted: 27 June 2018 . Published Online: 24 July 2018

Keith E. Whitener

## COLLECTIONS

Paper published as part of the special topic on [Special Issue on 2D Materials](#)

<sup>EP</sup> This paper was selected as an Editor's Pick



View Online



Export Citation



CrossMark

## ARTICLES YOU MAY BE INTERESTED IN

[Review Article: Stress in thin films and coatings: Current status, challenges, and prospects](#)  
Journal of Vacuum Science & Technology A **36**, 020801 (2018); <https://doi.org/10.1116/1.5011790>

[Review Article: Atomic layer deposition for oxide semiconductor thin film transistors: Advances in research and development](#)  
Journal of Vacuum Science & Technology A **36**, 060801 (2018); <https://doi.org/10.1116/1.5047237>

[Graphene and related two-dimensional materials: Structure-property relationships for electronics and optoelectronics](#)  
Applied Physics Reviews **4**, 021306 (2017); <https://doi.org/10.1063/1.4983646>



**HIDEN**  
ANALYTICAL

## Instruments for Advanced Science

Contact Hiden Analytical for further details:  
**W** [www.HidenAnalytical.com](http://www.HidenAnalytical.com)  
**E** [info@hiden.co.uk](mailto:info@hiden.co.uk)

[CLICK TO VIEW](#) our product catalogue

**Gas Analysis**

- dynamic measurement of reaction gas streams
- catalysis and thermal analysis
- molecular beam studies
- dissolved species probes
- fermentation, environmental and ecological studies

**Surface Science**

- UHV/TPO
- SIMS
- end point detection in ion beam etch
- elemental imaging - surface mapping

**Plasma Diagnostics**

- plasma source characterization
- etch and deposition process reaction kinetic studies
- analysis of neutral and radical species

**Vacuum Analysis**

- partial pressure measurement and control of process gases
- reactive sputter process control
- vacuum diagnostics
- vacuum coating process monitoring



# Review Article: Hydrogenated graphene: A user's guide

Keith E. Whitener, Jr.<sup>a)</sup>

Chemistry Division, U.S. Naval Research Laboratory, 4555 Overlook Ave., SW, Washington, DC 20375

(Received 11 April 2018; accepted 27 June 2018; published 24 July 2018)

Graphene's chemical versatility is unique among two-dimensional materials. One of the simplest and most well-studied chemical modifications of graphene is hydrogenation. The electronic, optical, and mechanical properties of hydrogenated graphene can differ significantly from those of unmodified graphene, and the tunability of these properties has played a major factor in the broad interest in hydrogenated graphene throughout the scientific community. Here, the author presents a practical review of the state of the art in hydrogenated graphene research. The target audience is the researcher who is interested in working with hydrogenated graphene but lacks practical experience with the material. The author focuses on considerations of the working scientist, highlighting subtleties in preparation and characterization that are generally only gained by experience in the laboratory. In addition, the author enumerates a number of the most important categories of results concerning the properties of hydrogenated graphene. In particular, the author examines what these results mean for potential near- and long-term applications of hydrogenated graphene. © 2018 Author(s). All article content, except where otherwise noted, is licensed under a Creative Commons Attribution (CC BY) license (<http://creativecommons.org/licenses/by/4.0/>).  
<https://doi.org/10.1116/1.5034433>

## I. INTRODUCTION

Graphene, a two-dimensional hexagonal carbon material, has received a wealth of attention since its isolation in 2004.<sup>1</sup> Its discovery inspired the study of a wide variety of novel two-dimensional materials, many of which have remarkable electronic, magnetic, mechanical, and optical features which do not appear in their bulk counterparts. As extensively as their physical properties have been explored, the chemistry of most of the known 2D materials remains significantly underdeveloped. Graphene is the sole exception to this rule: in spite of graphene's relative chemical inertness, researchers have discovered and advanced a wide variety of reaction motifs on graphene.

Chemically modified graphene (CMG) often has significantly different properties from the parent material, and CMGs bearing different functionalities have different properties from each other as well. This chemical approach to generating custom functionality in graphene is in stark contrast to the relative inflexibility of properties in nongraphene 2D materials. For example, if one wishes to change the band gap in 2D molybdenum disulfide, one must change the fundamental nature of the material, either by altering the transition metal or by altering the chalcogen. For graphene, on the other hand, changing electronic properties can be achieved by chemically functionalizing the graphene, rather than building a new 2D material from scratch. Thus, the ability to alter graphene via chemistry corresponds to the ability to generate a group of 2D materials with a large variety of properties in a far simpler and more systematic way than currently exists in nongraphene 2D materials.

Even though the chemistry of graphene has been extensively developed—including the functionalization of bulk graphite before the isolation of the pristine 2D material itself—the most useful chemistries can be grouped into a few broad categories. These include various oxidation schemes, halogenation reactions, hydrogenation and alkylation reactions, and reactions with diazonium salts and other reactive organic species.<sup>2</sup> The most extensively studied of these is the production of graphene oxide, which results in a complex product bearing heterogeneous oxygen functionalities (alcohol, epoxy, carboxyl, etc.) and which is notable for its ability to be further chemically modified to give a vast array of potential products.<sup>3</sup> Somewhat less well-advertised is the fact that the other chemistries (halogenation, hydrogenation, and diazonium reaction) share this property of accommodating further chemical modifications. These secondary modifications carry an additional advantage in that they allow only one type or very few types of functionality, indicating that, at least in principle, the products should be easier to characterize.

In contrast, hydrogenation represents the simplest possible chemical modification of graphene. Assuming no breakage of carbon-carbon bonds, only one hydrogen can bond to each lattice carbon. Interestingly, one would expect that, based on the similar electronegativities of carbon and hydrogen and prior experience with C-H bonds in organic chemistry, the C-H bond would be nonpolar, not disrupting the doping of the graphene significantly. In addition, in organic molecules, the C-H bond is quite unreactive, so one would expect hydrogenated graphene to be quite stable and chemically inert. At least at the outset, hydrogenated graphene was expected to be a chemically robust, nonpolar two-dimensional material that could see use in electronics and

<sup>a)</sup>Electronic mail: keith.whitener@nrl.navy.mil

possibly hydrogen storage.<sup>4</sup> That these two presuppositions turn out not to be true<sup>5–8</sup> makes the study of hydrogenated graphene that much more interesting.

In this practical review, we present a breadth of results from research on hydrogenated graphene that reveals a startling complexity concealed in this ostensibly simple material system. Our target audience is the researcher who is interested in hydrogenated graphene, but does not have the experience that comes from working directly on the material. We begin by reviewing the most important preparation methods. We note that graphene is quite chemically unreactive, requiring either that graphene or hydrogen be chemically activated in order to form hydrogenated graphene. We then move on to a brief survey of characterization methods, outlining the most useful methods and their capabilities and limitations in revealing information about graphene modification. Finally, we assess the physical and chemical properties of hydrogenated graphene and their applications.

In contrast with earlier reviews on hydrogenated graphene,<sup>9–11</sup> this work focuses almost exclusively on experimental results, rather than theoretical modeling. Theoretical results are introduced only to explain or clarify experimental findings. We include a wide range of experimental results in preparation, characterization, and application to represent the breadth of the current effort on hydrogenated graphene. In addition, we highlight a number of disagreements and discrepancies in the literature on hydrogenated graphene. Throughout the literature, there exist more than a few cases where reputable sources present results at odds with one another. As with any research topic that draws enormous amounts of interest, a plethora of results regarding hydrogenated graphene have accumulated within a very short period of time. The ISI Web of Science database reveals that about 200 papers per year are published on hydrogenated graphene or graphane, garnering around 6000 citations per year and climbing (Fig. 1). Since hydrogenated graphene is so new, and since results are generated so quickly, subtle differences in experimental approaches between research groups can often go unnoticed but lead to divergent observations. One example is the doping discrepancy observed between Elias *et al.*<sup>12</sup> and Matis *et al.*<sup>5</sup> Elias *et al.* observed that hydrogenated graphene was quite heavily p-doped relative to pristine graphene, whereas Matis *et al.* observed that hydrogenated graphene was slightly n-doped relative to pristine graphene. The issue was

resolved by Matis *et al.*, who showed that the p-doping effect was caused by physisorbed water and that dry hydrogenated graphene was n-doped. Our own group later corroborated this effect.<sup>13</sup> For a researcher who is embarking on the study of hydrogenated graphene for the first time, these discrepancies in the literature can be very difficult to navigate. One of the goals of this practical review is to elucidate some of the areas where small, subtle changes in experimental procedure can lead to remarkably different results.

An important note about terminology: One often finds studies of graphane (fully hydrogenated graphene) and hydrogenated graphene with crystalline order in the theoretical literature. We must point out, following the 2013 review by Pumera and Wong,<sup>9</sup> that fully hydrogenated graphene has not yet conclusively been observed experimentally. A wealth of papers observe that graphene typically hydrogenates inhomogeneously, in “patches.”<sup>7,14,15</sup> One exception to this rule is when the substrate imposes some type of highly ordered Moire pattern on the electronic structure of the graphene above, as observed first by Balog *et al.* (see Sec. II F for more detail).<sup>16</sup> We also mention that researchers sometimes use the terms “graphane” or “hydrogenated graphene” to refer to hydrogenated graphenelike material, such as hydrogenated graphene oxide or graphene fluoride. In these cases, there will often be multiple functionalities present in the hydrogenated material. It is important in these cases to pay attention to how the material is synthesized and characterized to put the results of such studies into the proper context.

## II. PREPARATION

As mentioned earlier, graphene is quite chemically inert and requires rather powerful reagents to effect any sort of chemical change. This is reflected in the well-known preparation of graphene oxide—requiring *in situ* generation of the extremely powerful oxidizer manganese (VII) oxide—as well as halogenation and diazotization of graphene, both of which require the generation of highly reactive radical species. Graphene's inertness is anticipated in the inertness of benzene. The extensive aromatic network in graphene presents a highly electronically homogeneous surface, the symmetry of which must be broken as a first step in any reaction. The formation of a chemical bond with graphene changes the geometry of the carbon at the reaction site from  $sp^2$  trigonal planar to  $sp^3$  pyramidal, straining the rest of the hexagonal lattice.<sup>4</sup>

These considerations apply in the case of hydrogen as well as any other reactive species. A number of preparative routes to hydrogenated graphene have been demonstrated since its initial production in 2009.<sup>12</sup> All of them require either activation of hydrogen (H-activation) or activation of the graphene lattice (C-activation) in order to render the reaction viable. We focus on the four most prominent of these routes: plasma hydrogenation, thermal cracking of hydrogen, dissolving metal reduction, and electrochemical hydrogenation. We have also included a table (Table I) for easy reference covering various important features of each of these four methods.

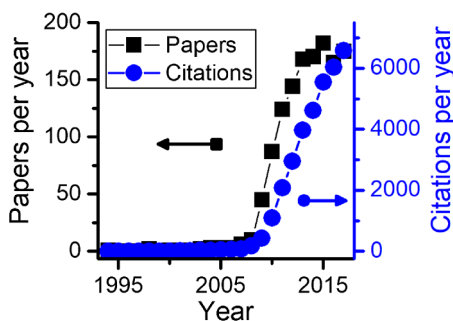


FIG. 1. Number of papers and citations per year for hydrogenated graphene and graphane. Data were taken from ISI Web of Science.

TABLE I. Comparison of four common methods of preparing hydrogenated graphene.

Method	Features	Advantages	Disadvantages
Plasma hydrogenation	<ul style="list-style-type: none"> <li>Hydrogen plasma applied to graphene (Ref. 12)</li> <li>Physical process</li> <li>H-activated</li> </ul>	<ul style="list-style-type: none"> <li>Clean, only involves C and H</li> <li>Safe, enclosed system</li> <li>Highly tunable reaction parameters (Refs. 17, 18)</li> </ul>	<ul style="list-style-type: none"> <li>Can only do single/few layer graphene (Ref. 19)</li> <li>Requires specialized equipment (Refs. 20, 21)</li> <li>Hydrogenation not as extensive as other methods (Refs. 12, 17)</li> <li>Prolonged exposure can damage graphene (Refs. 22–24)</li> </ul>
Thermal cracking	<ul style="list-style-type: none"> <li>Thermally generated atomic hydrogen applied to graphene (Refs. 25, 26)</li> <li>Physical process</li> <li>H-activated</li> </ul>	<ul style="list-style-type: none"> <li>Clean, only involves C and H</li> <li>Usually very safe</li> <li>Can be performed <i>in situ</i> alongside microscopy analysis (Refs. 25, 27)</li> </ul>	<ul style="list-style-type: none"> <li>Can only do single/few layer graphene (Ref. 26)</li> <li>Usually requires specialized equipment (Ref. 25)</li> </ul>
Dissolving metal reduction	<ul style="list-style-type: none"> <li>Solvated electrons activate graphene to proton uptake (Refs. 15, 28)</li> <li>Chemical process</li> <li>C-activated</li> </ul>	<ul style="list-style-type: none"> <li>Can handle bulk quantities (Refs. 28–30)</li> <li>Can obtain very high levels of hydrogenation (Ref. 31)</li> <li>Not limited to hydrogen functionality (Refs. 13, 32, 33)</li> </ul>	<ul style="list-style-type: none"> <li>Numerous safety considerations</li> <li>Reaction parameters not easily tunable (Refs. 13, 15)</li> </ul>
Electrochemical reduction	<ul style="list-style-type: none"> <li>Negative potential activates graphene to proton uptake (Ref. 34)</li> <li>Chemical process</li> <li>C-activated</li> </ul>	<ul style="list-style-type: none"> <li>Can handle bulk quantities (Ref. 35)</li> <li>Can obtain moderately high levels of hydrogenation (Refs. 35, 36)</li> <li>Reaction parameters are tunable (Refs. 34, 35)</li> <li>Generally safe</li> <li>Not limited to hydrogen functionality (Ref. 37)</li> </ul>	<ul style="list-style-type: none"> <li>Can introduce chemical impurities (Refs. 35, 37)</li> <li>Unforeseen side reactions are possible (Refs. 35, 36)</li> </ul>

## A. Plasma hydrogenation

One of the most extensively developed routes to hydrogenated graphene involves exposure of graphene to a hydrogen/argon plasma, initially introduced by Elias *et al.*<sup>12</sup> In this case, hydrogen gas is activated via electric discharge or applied RF field to form a reactive plasma. Graphene, upon exposure to this plasma, takes up hydrogen adatoms to give hydrogenated graphene. It is also worth mentioning that plasma treatment can be extended beyond simple hydrogenation: oxidation, nitrogenation, and fluorination of graphene have all been achieved via plasma treatment.<sup>38</sup>

There has been some debate over what the exact hydrogenating species are. Jones *et al.* argued that the energetic electrons in the plasma cause the fragmentation of physisorbed water and subsequent hydrogenation of the graphene.<sup>21</sup> They support this statement by annealing graphene at high temperatures to drive off water and then observing that the hydrogen plasma does not induce a large number of defects, as observed by Raman spectroscopy. However, Wojtaszek *et al.* argue that adsorbed water is not responsible for hydrogenation, at least under the conditions they examine. They base their conclusion on the fact that ion bombardment from an argon plasma does not increase defect density in graphene, whereas bombardment with an H<sub>2</sub>/Ar plasma does increase defect density. They argue that the adsorbed water layer should be present in both cases, and that the argon ions have

plenty of energy to fragment this water layer, so the nonobservation of defect density leads them to conclude that the water layer is not required for hydrogenation.

Alternatively, Felten *et al.* assert that the main hydrogenating species are H<sup>+</sup>, H<sub>2</sub><sup>+</sup>, and H<sub>3</sub><sup>+</sup>. They monitor the energy distributions and abundances of these species, showing that different locations within the plasma chamber have dramatically different local chemistries.<sup>17</sup> This finding provides a possible resolution to the disagreement between the studies of Jones *et al.* and Wojtaszek *et al.* Wojtaszek *et al.* used a reactive ion etching setup, where the plasma was generated in a parallel plate electrode configuration and the graphene was mounted directly on one of the plates [Fig. 2(a)].<sup>20</sup> On the other hand, Jones *et al.* used a remote setup, where the plasma was generated approximately 15 cm from the graphene sample [Fig. 2(b)].<sup>21</sup> The difference in experimental configurations leads to different local plasma temperatures as well as different sample biases. Methodological subtleties such as these, which lead to large discrepancies in experimental outcomes, are a common theme in hydrogenated graphene research.

There are two major advantages of plasma hydrogenation over wet chemical methods. First, the chemical species in the reaction are particularly simple: carbon (from the graphene) and hydrogen. Thus, there is very little risk of contamination of the graphene with other elements. In contrast, there have at times been questions about the purity of hydrogenated graphene obtained via wet chemical means. For example, x-ray

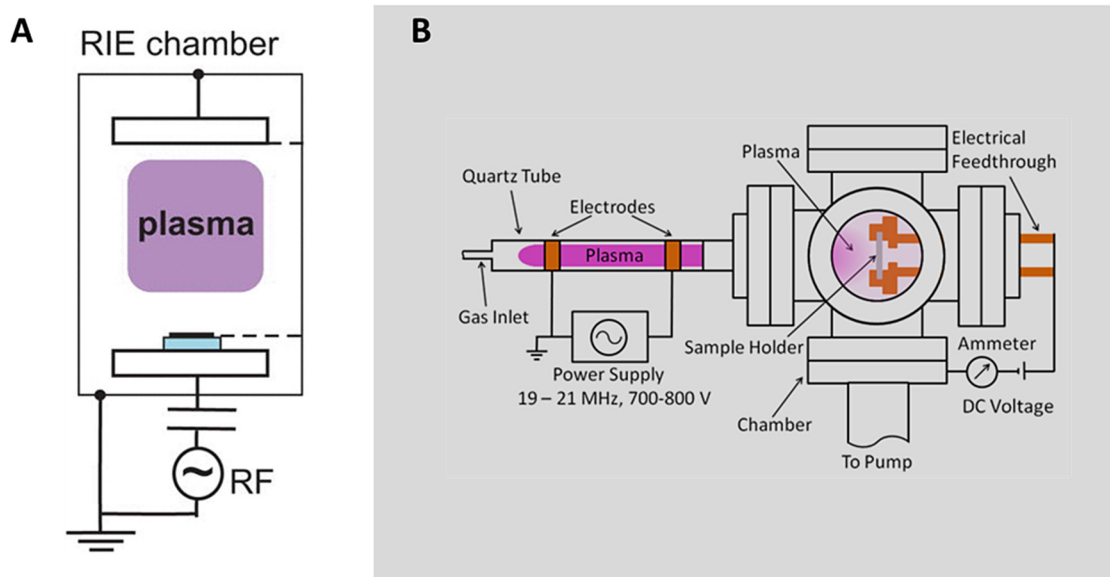


Fig. 2. (a) Graphene hydrogenation reaction schematic in the direct plasma RIE chamber used by Wojtaszek *et al.* Adapted from Ref. 20 with permission from AIP Publishing. (b) Graphene hydrogenation setup in the remote plasma configuration used by Jones *et al.* Reprinted from Ref. 21 with permission from AIP publishing.

photoelectron spectroscopy (XPS) of bulk graphite derivatives obtained via wet chemical hydrogenation reveals the presence of species that are not carbon or hydrogen, raising the possibility of nonhydrogenative side reactions.<sup>29,31,39</sup> Second, plasma methods are fine-tunable. The energy, temperature, composition, and electric field configuration can all be altered to fine-tune the coverage of hydrogen atoms on the graphene.<sup>18</sup>

One important experimental consideration for the plasma hydrogenation of graphene is that one cannot obtain a product which is as heavily hydrogenated as what can be achieved using other methods. The limiting factor is the competition between the rate at which the material hydrogenates and the rate at which the plasma begins to irreversibly etch and damage the graphene. Even at low energies, hydrogen plasma will cause sputtering defects such as vacancies and dislocations to form, and these defects will eventually predominate over the hydrogen adatoms.<sup>17,22-24</sup> Another important consideration is the need for specialized plasma equipment. This requirement is not prohibitive for research facilities where a significant amount of microfabrication research occurs, as most of these facilities will have access to plasma chambers and the necessary equipment. However, plasma hydrogenation is not as easily accessible as other methods covered herein.

## B. Thermal cracking

Some of the first experimental observations of hydrogenated graphene in 2009 used a hot ( $\sim 1400^\circ\text{C}$ ) tungsten filament to crack hydrogen gas into atomic hydrogen, to which they subsequently exposed epitaxial graphene on SiC(0001) (Fig. 3).<sup>25-27</sup> These groups observed the reaction product using scanning tunneling spectroscopy and showed for the first time that individual hydrogen adatoms have an outside

effect on the local density of states extending several angstroms from the atomic site. Bostwick *et al.* also postulated that the observed metal-to-insulator transition upon hydrogenation is due to localization effects, a fact which we will discuss in Sec. IV A.<sup>27</sup>

Thermal cracking has the same advantage as plasma hydrogenation in that the only species involved in the reaction are the graphene and atomic hydrogen. Thus, the hydrogenated graphene is ensured to be elementally “clean” at the time of synthesis. However, there has been some concern that the hydrogen atoms coming from a  $1400^\circ\text{C}$  hot filament could be energetic enough to damage the basal plane of the graphene. Zheng *et al.* attempted to address these concerns by first flowing  $\text{H}_2$  gas over a nickel catalyst, which homolytically dissociated the gas into atomic hydrogen at a lower temperature of  $820^\circ\text{C}$ .<sup>40</sup> The material that they obtained from this reaction was observed to be superhydrophobic, with a water contact angle of  $\sim 140^\circ$ .

Thermal cracking is a very effective and clean method of hydrogenation. However, like plasma hydrogenation, it

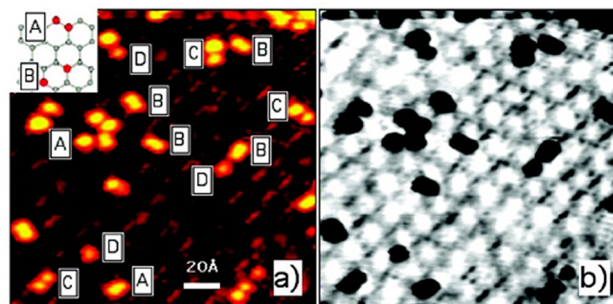


Fig. 3. (a) STM image of hydrogen adatoms on epitaxial graphene on SiC. (b) Color-reversed image to show underlying alignment of crystallographic directions in graphene. Reprinted from Ref. 25 with permission from the American Chemical Society.

requires specialized equipment—in particular, a vacuum chamber setup where a precisely controlled atmosphere of hydrogen gas can be exposed to a hot filament—and this requirement makes it less accessible to general researchers than the wet chemical methods described below. Nonetheless, thermal cracking and plasma hydrogenation together make up the principal methods where the hydrogen—not the graphene—is activated toward reaction.

### C. Dissolving metal reduction

*Note: Dissolving metal reductions present a number of important safety considerations. We advise the reader to review our discussion of these considerations in Sec. II F as well as other relevant protocols before attempting any of these reactions.*

Dissolving metal reductions have been used for hydrogenation reactions in organic chemistry for nearly 70 years.<sup>41</sup> The classic example of this reaction is the Birch reduction, which involves combining lithium metal with liquid ammonia. The lithium dissociates into  $\text{Li}^+$  and solvated electrons,  $e^-$ . In this case, in contrast with the plasma or thermal methods, it is the graphene—and not the hydrogen—which is activated in the reaction: Graphene is introduced into the lithium/ammonia mixture, and the electrons activate graphene toward reaction with electrophilic species (Fig. 4).

Most of the conditions of the dissolving metal reduction are variable. Thus, we see a panoply of results in the literature where the metal, solvent, proton source, and even starting material are varied.<sup>42</sup> Typical choices for metal include the alkali metals as well as the alloy NaK. The original solvent, liquid ammonia, boils at  $-33^\circ\text{C}$  and is therefore more difficult to work with than solvents which are liquid at room temperature. Thus, a number of groups have explored room-temperature reactions with tetrahydrofuran, diethyl ether, and ethylenediamine as solvents.<sup>29,43</sup> The proton source is almost always either water or an alcohol.<sup>31,44</sup> The starting material is generally either supported single-to-few-layer graphene or graphite,<sup>13,28,29</sup> but increasingly, researchers have begun to

examine functionalized graphenes and graphites as starting materials. Zhang *et al.*<sup>45</sup> and Yang *et al.*<sup>31</sup> found a high degree of hydrogenation using the Birch reduction on fluorinated graphite. Papadakis *et al.* applied sodium borohydride, a different reducing agent, to fluorinated graphite to obtain partially fluorinated and hydrogenated graphene.<sup>46</sup> Eng *et al.*<sup>39</sup> and Subrahmanyam *et al.*<sup>47</sup> used graphite oxide as a starting material in the Birch reduction to obtain final products which exhibited intriguing magnetic properties and promising hydrogen storage properties, respectively.

Dissolving metal reductions can be subject to more subtle variations that nevertheless lead to divergent observations. In our own group, we found that bilayer and few-layer graphene was highly hydrogenated after only 2 min in liquid ammonia with lithium as the reducing agent and ethanol as the proton donor.<sup>7</sup> Yang *et al.* found similar results using *tert*-butanol as the proton donor in the hydrogenation of bulk graphite.<sup>28</sup> However, Zhang *et al.* found that methanol was not effective in hydrogenating bilayer graphene, even after 1 h of reaction.<sup>15</sup> No trend in  $\text{pK}_a$  of the proton donor or steric effect explains this discrepancy. The crucial difference in the experiments was the amount of time the proton donor was allowed to react with the graphene in the presence of active lithium. In our own group's case, the lithium and proton donor were combined before the graphene was added to the reaction. In the case of Yang *et al.*, the proton donor was allowed to react in the presence of the lithium for 60 min. In the case of Zhang *et al.*, however, the proton donor was used to quench the reaction, meaning that the amount of time that the proton donor was active along with the lithium was limited (to what extent is unclear, but the time both lithium and proton donor were active could be as little as a few seconds). Our group had observed a similar—though unreported at the time—effect in partially hydrogenating graphene for magnetic experiments, where we used the proton donor to quench the reaction very quickly.<sup>48</sup> Thus, in all cases, the lithium had plenty of time to intercalate between layers, but the proton did not have time to intercalate when the reaction was quickly quenched.

One is not constrained to use proton donors to quench the Birch reduction. Various groups have shown that the same reductive coupling procedure can be used to alkylate or arylate graphene or add heteroatoms. In the case of alkylation, the proton donor is generally replaced by an alkyl halide.<sup>32,33,49</sup> In the case of arylation, the reaction generally proceeds via coupling between an aryldiazonium salt and the reduced graphene.<sup>32,33</sup> Heterofunctionalities like stannylation can be added to graphene by replacing the proton donor with tributyltin chloride.<sup>13</sup> In any case, the ability to extend the Birch reduction beyond hydrogen functionalization to organic functionalization is a direct result of the fact that the graphene, rather than the hydrogen, is the activated species in the reaction.

### D. Electrochemical reduction

Of all the methods of hydrogenation, electrochemical reduction is likely the most universally accessible. It requires

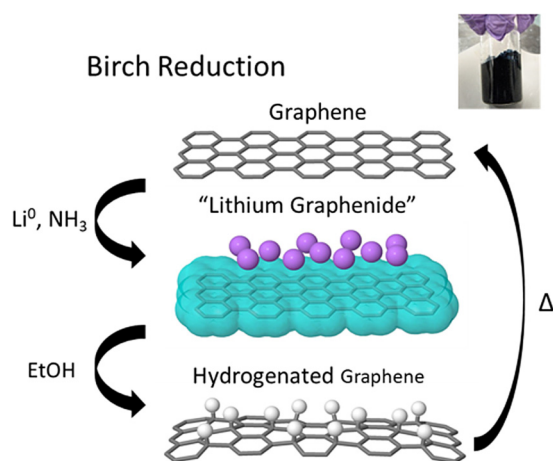


FIG. 4. Schematic of the dissolving metal Birch reduction of graphene to hydrogenated graphene. Inset: characteristic blue color of solvated electrons in ammonia. Adapted from Ref. 13 with permission from Elsevier.

a minimum of specialized equipment and essentially no chemicals which are nonstandard or difficult to handle. Graphene can be electrochemically reduced with hydrogen as well as various alkyl functionalities. The chemistry in electrochemically mediated reduction of graphene is similar to the above-described case of chemically mediated reduction. In this case, graphene serves as a cathode in an electrochemical cell. A potential is applied across the electrodes and electron density accumulates on graphene. This increased electron density activates graphene toward uptake of electrophilic reagents.

Several groups had observed electrochemical hydrogenation of graphene before conclusively determining that the graphene was being hydrogenated. Wang *et al.* used a cathodic potential to exfoliate few-layer graphene sheets from graphite, but they did so in an aprotic environment, so they did not observe significant covalent functionalization of graphene.<sup>50</sup> Su *et al.* performed electrochemical exfoliation in a solution of H<sub>2</sub>SO<sub>4</sub>, observing heavily functionalized graphene which lost most of its functionality upon exposure to intense laser light. However, they incorrectly attributed this functionalization to oxidation by the sulfuric acid.<sup>36</sup> Daniels *et al.* were among the first to unequivocally state that electrochemistry could add hydrogen to the graphene lattice.<sup>34</sup> However, they misidentified a Raman peak at 2930 cm<sup>-1</sup> as a C-H stretch peak, when in fact it is the D + D' combination band, as revealed by dispersion experiments (as well as comparing the Raman spectrum of hydrogenated to deuterated graphene, where no isotope shift is observed). Zhao *et al.* showed unmistakable evidence of hydrogenation by finding the C-H stretching peaks in the infrared spectrum, putting the issue to rest.<sup>35</sup>

The electrochemical method employed by Zhao *et al.* used highly oriented pyrolytic graphite as a cathode. A high potential (20 V) was used to effect both reaction and exfoliation. This potential is far higher than what is required to electrolyze water, so the electrolytic system used was nonaqueous. In this case, the researchers used 0.1M tetrabutylammonium hexafluorophosphate dissolved in *N,N*-dimethylformamide. It is likely that the hydrogen comes from some high-potential electrolytic reaction of the solvent or possibly trace amounts of water in the system.<sup>35</sup> Daniels *et al.* used a cathode of epitaxial graphene grown on SiC instead of graphite. Their electrolyte was 10% H<sub>2</sub>SO<sub>4</sub> in water, and they used a much lower potential of 1 V to avoid electrolysis of water and production of hydrogen at the cathode.<sup>34</sup>

We emphasize that electrochemistry can reductively couple moieties besides hydrogen to graphene, including aryl diazonium salts.<sup>37</sup> This is exactly in analogy with reductive coupling of groups to alkali-metal doped graphene considered in Sec. II C. In these cases, the electrolyte must be strictly aprotic to rule out the possibility of hydrogenation masquerading as some other functionality. In general, electrochemical functionalization (hydrogen or otherwise) requires four elements: a voltage source, a graphene/graphite cathode, an electrolyte, and a functional group—sometimes the electrolyte doubles as the functional group, as in the case

of water; sometimes they are separate species. These four elements, being easy to obtain and simple to work with, make electrochemistry quite accessible for a scientist who is just beginning to work with hydrogenated graphene.

## E. Other methods

Most other hydrogenation methods are either quite specialized or require exotic setups. We mention several of them here to give a sense of the variety of approaches taken to produce hydrogenated graphene. Sofer *et al.* explored hydrogenation and deuteration of graphene oxide using the Clemmensen reduction.<sup>51,52</sup> They found that the zinc/HCl couple could reduce ketone and epoxide groups on graphene to sp<sup>3</sup> hydrogen adatom sites. Ryu *et al.* was one of the first groups to report evidence of graphene hydrogenation by electron irradiation of hydrogen silsesquioxane, a common reagent in photolithography and e-beam lithography.<sup>53</sup> This method presents a major advantage over other methods by being potentially patternable. The drawback was that the material obtained from the reaction was very minimally hydrogenated. Chen *et al.* produced hydrogenated graphene from a suspension of graphene oxide in water via irradiation from a <sup>60</sup>Co gamma ray source.<sup>54</sup> This reaction presumably proceeds via solvated electrons generated from the interaction of the gamma ray with water, in a manner mechanistically similar to the dissolving metal reduction. Kintigh *et al.* produced hydrogenated graphene via reaction of graphite with pentaethylhexamine at 380 °C.<sup>55</sup> Tjung *et al.* produced crystalline nanodomains of hydrogenated graphene by using the current from a scanning tunneling microscope (STM) tip to homolytically cleave physisorbed molecular hydrogen on graphene.<sup>56</sup> Byun *et al.* performed a similar experiment using a conductive atomic force microscope (AFM) tip and ambient humidity as the proton source.<sup>57</sup>

## F. Further considerations

We have noted throughout this review that to induce a reaction between graphene and hydrogen, one must activate either the graphene or the hydrogen. At this point, we must point out that the reactivity of graphene, being only one atom thick, can be heavily influenced by the substrate on which it sits. Researchers have noted that the reactivity of graphene toward diazonium species and fluorine depends on what underlies graphene.<sup>58,59</sup> In general, electronically heterogeneous metal oxides make graphene more reactive, while metals and other highly electronically homogeneous surfaces make graphene less reactive. This difference in reactivity is attributable to the perturbation of the graphene electronic structure by the substrate. Heterogeneous substrates cause the formation of electron-hole “charge puddles,” which break the electronic symmetry of the graphene lattice and allow chemical bonding to occur more favorably than in systems with homogeneous substrates.<sup>58</sup>

Hydrogenation presents an interesting test case for the idea of charge puddles mediating graphene reactivity. Choice of substrate is tantamount to mild activation or deactivation

of the graphene, but if the graphene is already strongly activated (either chemically or electrochemically), this activation should swamp any substrate effect for hydrogenation. On the other hand, if we choose only to activate the hydrogen (as in plasma treatment or thermal cracking), the substrate effect should be observable, since it is the only activating or deactivating perturbation of graphene itself. Since we can choose reaction conditions where either hydrogen or graphene is independently strongly activated, we can test this hypothesis. In fact, Son *et al.*<sup>60</sup> found that plasma hydrogenation of graphene is strongly affected by whether the substrate is MoS<sub>2</sub> or hexagonal boron nitride. On the other hand, several groups have observed that the Birch hydrogenation and electroreduction of graphene proceed unimpeded in the presence of a number of normally activating and deactivating substrates.<sup>7,29,32</sup> Thus, choice of hydrogenation method plays a direct role in whether substrate effects on graphene reactivity will be observed or not.

The substrate effect is illustrated most vividly in the case where the graphene lattice is epitaxially incommensurate with its substrate, as when graphene rests on Ir(111) [Figs. 5(a) and 5(b)].<sup>16,62</sup> In this case, the interaction of graphene and iridium forms a hexagonal superlattice with a lattice constant of around 21 Å, where the graphene is alternately bent downward—strongly bound to the iridium substrate—and upward—free from substrate interactions. The iridium increases electron density on the graphene in the sites where the graphene and iridium are in closest contact. This activation renders the graphene more susceptible to plasma hydrogenation, and researchers observed via STM that indeed hydrogen adsorbs to graphene in a pattern dictated by the superlattice.<sup>16</sup>

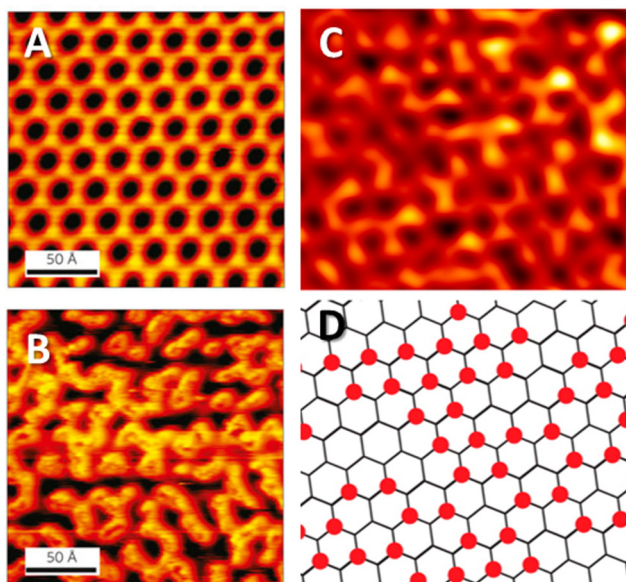


Fig. 5. (a) STM image of graphene on Ir(111) Moire pattern. (b) STM image of hydrogenation of graphene/Ir(111) shows that hydrogen functionalities preserve Moire pattern. (a) and (b) adapted from Ref. 16 with permission from Springer/Nature. (c) STM image and (d) schematic of crystalline nanodomains in hydrogenated graphene. (c) and (d) adapted from Ref. 61 with permission from the American Chemical Society.

Another important consideration in graphene hydrogenation, and one that it shares with other covalent functionalizations, is that it proceeds inhomogeneously over the material surface. In fact, functionalization of graphene seems to begin at a defect or edge site, where the carbon atoms are activated relative to those on the basal plane of the graphene. From there, the reaction spreads outward, with the presence of adatoms activating neighboring carbons to further reaction.<sup>15,59,63</sup> In the case of multilayer graphene, the functionalization often proceeds from the edges of the sheets inward.<sup>15</sup> The most homogeneous products are therefore generally either those obtained via very short reaction times (where the reaction sites appear largely stochastically) or those obtained after long reaction times (when the inhomogeneity has been smoothed out by further reactions).

Finally, safety is an important consideration in any chemical preparation. For the plasma and thermal methods, the hydrogenation apparatus is mostly contained and presents little danger when properly operated. However, plasma generators can run at high voltages and often require handling of compressed gas, both of which can be hazards if not attended to properly. Electrochemical hydrogenation requires handling of mildly dangerous chemicals such as dilute sulfuric acid. The electrochemical process itself can generate hydrogen gas, depending on the voltage at which the preparation is carried out. Thus, when performed on a large scale, this factor needs to be considered. The dissolving metal reduction requires special safety consideration. Because liquid ammonia boils to give off noxious vapors, all manipulations should be performed in a well-ventilated fume hood. In addition, liquid ammonia is cryogenic, requiring the use of a dry ice bath. If a closed manifold system is used, extreme care must be taken to prevent overpressurization of the manifold, an explosion risk. The alkali metal itself is water and air-sensitive, and care must be taken to prevent it from reacting vigorously or igniting. Finally, the quenching of the reaction is very exothermic, and must be done cautiously and slowly to prevent an uncontrolled reaction.

### III. CHARACTERIZATION

Among the chemically modified graphenes, hydrogenated graphene presents unique challenges for characterization. Surface coverage by other functionalities is typically quantified by XPS, but XPS cannot detect hydrogen atoms [Fig. 6(b)]. Hydrogen only has one electron to lose: a valence electron, and its photoelectron spectrum cannot be disentangled from the rest of the ultraviolet valence band photoelectron spectrum. In addition, the chemical shift in the carbon 1s XPS peak between graphene and hydrogenated graphene is too small to be a reliable quantitative indicator of surface functionalization.

Most other common measures of graphene functionalization (e.g., Raman spectroscopy) are not element-specific, and thus cannot provide a truly reliable measure of adatom surface coverage. The few exceptions have major caveats. For bulk graphite, one can perform elemental analysis to quantitatively determine hydrogen content,<sup>28,29,31,47,64</sup> but

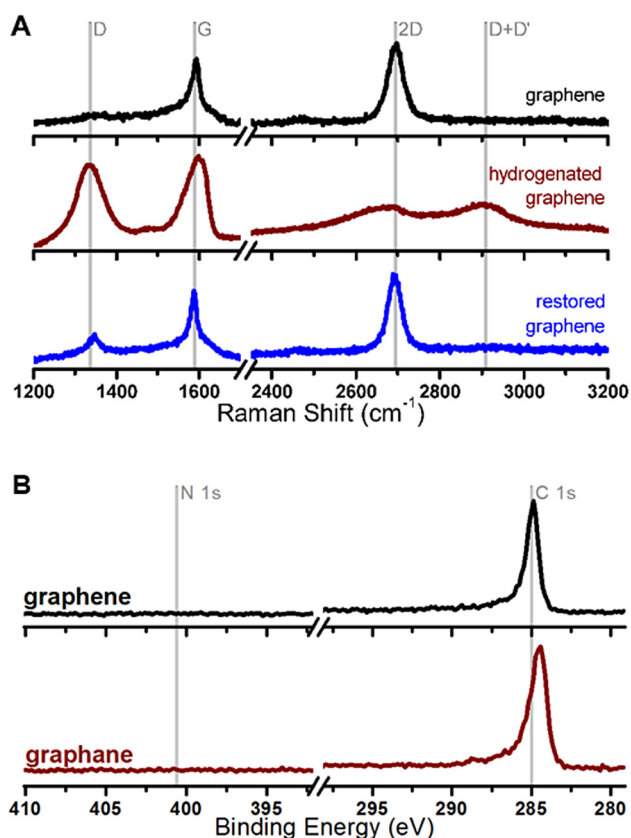


Fig. 6. (a) Raman spectra of graphene (top), Birch-hydrogenated graphene (middle), and thermally restored graphene (bottom). (b) XPS of graphene (top) and Birch-hydrogenated graphene (bottom). Adapted from Ref. 13 with permission from Elsevier.

this method is not sensitive enough to determine coverage of single- or few-layer graphenes. This method also cannot determine whether the observed hydrogen comes from chemisorbed adatoms on graphite or intercalated hydrocarbons left over from H-atom donors that have not been assiduously removed from the system. At least one group has had limited success using electron energy loss spectroscopy (EELS) to directly measure H-content,<sup>14</sup> but these results were performed inside a dedicated scanning transmission electron microscope, not a common or readily accessible technique. STM can provide an absolute measure of C/H ratio over a small area ( $>1 \mu\text{m}^2$ ), but the inhomogeneity of the hydrogenation process virtually ensures that such a small area will not be representative of the sample. Neutron scattering is another method that shows great promise in characterizing functionalized graphene, with a sensitivity toward hydrogen that is mediated by the ability to map a material's vibrational density of states.<sup>65,66</sup> However, neutron scattering experiments require access to a neutron source—almost always in the form of a dedicated facility—which is a barrier for widespread adoption of the technique. Therefore, the challenge of easily and precisely measuring hydrogen coverage over a large area on single or few-layer graphene supported on a surface remains an open problem.

Compounding this problem is the fact that highly hydrogenated graphene is unstable to the gradual loss of hydrogen

in ambient conditions.<sup>7</sup> This observation indicates that the bond from hydrogen to graphene is weak, and further complicates characterization via spectroscopic means. Several groups have observed that CMGs can be defunctionalized via photochemical or thermal excitation with a laser<sup>67–70</sup> or under the energetic beam of an electron microscope.<sup>48</sup> Hydrogenated graphene is therefore not only difficult to characterize with elemental specificity, but the product is often dynamic under the conditions of characterization. This requires the spectroscopist to use a gentle touch, so to speak. Accurate laser spectroscopy, for instance, involves use of low laser power and long integration times over many scans.

With all of these considerations in mind, we briefly survey several characterization methods that have been brought to bear on hydrogenated graphene. In particular, we discuss scanning probe methods (i.e., STM and AFM), particle scattering methods (i.e., electron microscopy and neutron scattering), and Raman spectroscopy.

### A. Scanning probe microscopy

While STM does not sample a large area of the graphene, it can still be very useful for determining local bonding configurations and changes in density of state induced by hydrogen. We noted earlier that fully hydrogenated graphene has yet to be produced, and we also note that crystalline partially hydrogenated graphene seems not to have been produced either. However, STM gives us a picture of the evolution of structure in increasingly hydrogenated graphene. For instance, Lin *et al.* used STM to observe crystalline nanodomains in hydrogenated graphene prepared by thermal cracking [Figs. 5(c) and 5(d)].<sup>61</sup> Gonzalez-Herrero *et al.* used STM to map the magnetic moments from individual hydrogen atoms on graphene.<sup>71</sup> STM is thus a powerful tool to understand the precise processes involved in hydrogenation at the nanoscale.

Atomic force microscopy and its variations [electrostatic force microscopy, magnetic force microscopy (MFM), etc.] provide useful tools for examining surface features of hydrogenated graphene. We mentioned in Sec. II E that conductive AFM was used to crack hydrogen gas at the nanoscale for forming hydrogenated graphene.<sup>57</sup> Friction force has also been used to eliminate hydrogen from hydrogenated graphene by shearing hydrogen atoms from the graphene basal plane using an AFM tip.<sup>72</sup> Our group has used magnetic force microscopy to examine magnetism in partially hydrogenated graphene.<sup>48</sup> There are few of these examples of specialized applications of AFM to hydrogenated graphene in the literature. In general, AFM is more a workhorse technique—mainly to show the presence of a single graphene layer—than an analytical technique to determine specific properties of hydrogenated graphene.

### B. Particle scattering methods

Electron microscopy has been a workhorse of graphene science since its inception. Scanning electron microscopy allows facile imaging of the sheetlike morphology of graphene,

while transmission electron microscopy (TEM) can resolve features of graphene at the atomic scale. The use of electron microscopy methods specifically to characterize hydrogenated graphene has a wealth of precedent as well. In 2009, Elias *et al.* compared the TEM electron diffraction pattern obtained from pristine graphene with that of plasma-hydrogenated graphene [Fig. 7(a)] and found a decrease in the lattice spacing of about 5%, which they attributed to geometric changes in the graphene upon exposure to hydrogen plasma.<sup>12</sup>

A few researchers have also used EELS to provide evidence for hydrogen adsorption on graphene. EELS, typically performed within an electron microscope, relies on the inelastic scattering of electrons with a material. Bangert *et al.* used EELS to observe a decrease in the intensity of the  $\pi$ -plasmon band of graphene as well as the appearance of hydrogenic and diamondlike features [Fig. 7(b)].<sup>14</sup> Yang *et al.* mapped the hydrogen in bulk Birch-hydrogenated graphite using EELS to assert that the hydrogenation occurs not only at the edges of the graphene sheets but also in the interior of the basal plane [Figs. 7(c) and 7(d)].<sup>28</sup> However, these results have been called into question, because the techniques cannot conclusively determine whether the hydrogen signal is coming from chemisorbed hydrogen on

graphene itself or from physisorbed hydrocarbons present as contaminants on the graphene surface.<sup>73</sup>

Low energy electron diffraction (LEED) is another electron scattering technique that has been applied to hydrogenation of graphene. In particular, high-temperature epitaxial growth of graphene on silicon carbide typically produces a strongly bound buffer layer of carbon before freestanding graphene is obtained. Riedl *et al.* showed that this buffer layer can be freed from the SiC substrate via exposure to thermally cracked hydrogen. They confirmed this via LEED, where they showed that the superstructure diffraction spots associated with the buffer layer disappear upon exposure to atomic hydrogen.<sup>74</sup>

Inelastic neutron scattering (INS) works on a similar principle to EELS, but typically probes the vibrational energy regime instead of the valence electronic energy regime. INS is particularly useful for probing hydrogenated graphene for two reasons. First, the incoherent scattering cross section of hydrogen is an order of magnitude larger than that of carbon. Second, INS is not constrained by the selection rules that limit Raman and infrared spectroscopy. As a result, an INS measurement typically returns a faithful profile of the hydrogen vibrational density of states of a material.<sup>65</sup> Cavallari *et al.* subjected graphene oxide to a flux of hydrogen gas at

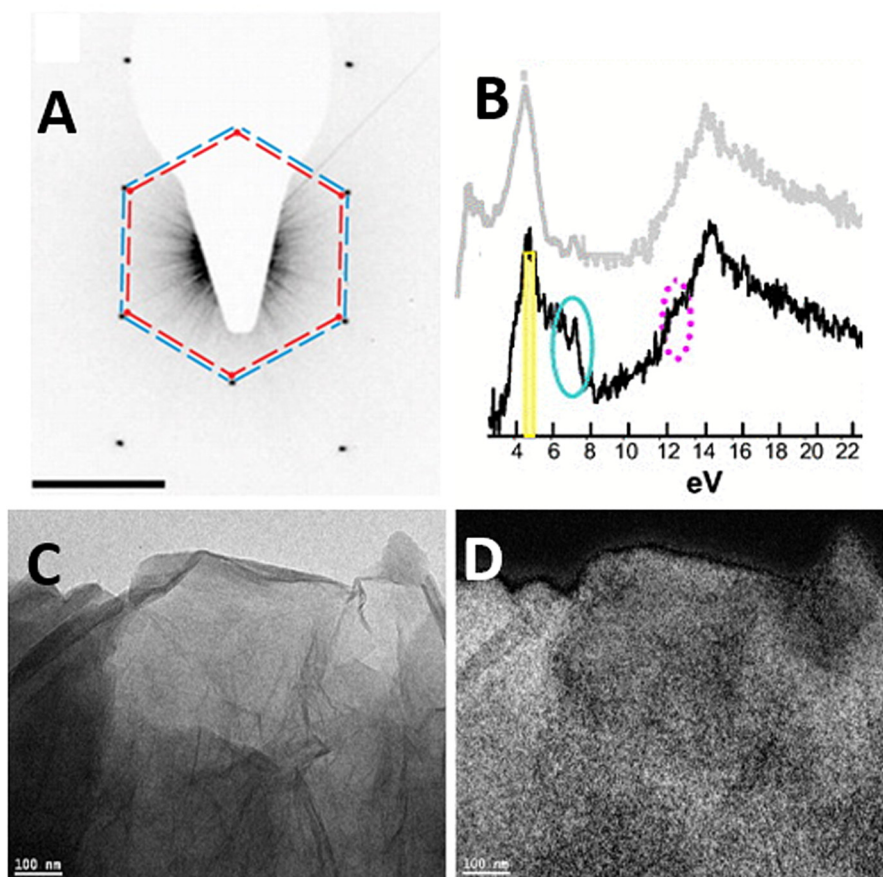


FIG. 7. (a) TEM diffraction pattern of graphene (inner dashed hexagon) and hydrogenated graphene (outer dashed hexagon) showing the decrease in lattice spacing due to hydrogenation. Scale bar is  $5 \text{ nm}^{-1}$ . Adapted from Ref. 12 with permission from AAAS. (b) EELS spectra of graphene (gray) and hydrogenated graphene (black), showing a diamondlike feature at 7 eV and a hydrogenic feature at 13 eV. Adapted from Ref. 14 with permission from AIP Publishing. (c) TEM image and (d) EELS hydrogen map of hydrogenated graphene. Scale bar is 100 nm. Adapted from Ref. 28 with permission from the American Chemical Society.

800 °C and measured the hydrogen density of states via INS. They observed the presence of C-H bending modes in one study,<sup>65</sup> and in another study were able to show that the hydrogen accumulated at edges and vacancies in the highly defective graphene oxide.<sup>75</sup> Another INS study by Natkaniec *et al.* confirmed the presence of hydrogens at the edges of graphene oxide treated with supercritical isopropanol.<sup>76</sup> Hydrogenated graphene (rather than graphene oxide) has yet to be examined via INS, but the technique seems to hold a significant degree of promise.

### C. Raman spectroscopy

The main spectroscopic tools for characterizing hydrogenated graphene are Raman spectroscopy, infrared spectroscopy, UV-visible spectroscopy, and XPS. We have mentioned that XPS is not particularly useful for studying hydrogenated graphene, because the chemical shift of the C 1s peak is negligible in going from sp<sup>2</sup> graphene to sp<sup>3</sup> hydrogenated graphene. Infrared spectroscopy reveals the presence of C-H or C-D bond stretches, but the signal is very weak and this measurement can only be performed reliably on bulk samples of hydrogenated graphene.<sup>28,29</sup> UV-visible spectroscopy provides a reliable measurement of the optical band gap and will be discussed in Sec. IV C.

The Raman spectra of graphene and its variants have been well studied [Fig. 6(a)].<sup>77</sup> In pristine graphene, the most prominent features are the first-order G peak at 1590 cm<sup>-1</sup> and the second-order 2D peak at 2680 cm<sup>-1</sup>.<sup>78,79</sup> The most important feature for the study of hydrogenated graphene is the D peak at around 1340 cm<sup>-1</sup>. This peak represents an intervalley scattering process near the K point of the Brillouin zone. The scattering process itself violates the conservation of momentum in the system, and therefore is strongly forbidden in pristine graphene. However, the presence of defects relaxes the momentum conservation requirements and upon introduction of defects, the D peak becomes quite prominent, even dominant for a range of hydrogen coverages.<sup>80,81</sup> These considerations make the D peak an excellent indicator of the progress of graphene hydrogenation.

At the same time, it must be noted that the evolution of the D peak with respect to defect density is not monotonic.<sup>80,81</sup> For very high levels of functionalization, the ratio of D peak to G peak intensity actually reaches a maximum and begins to decrease. In this regime, it is useful to have other consistently monotonic metrics to examine the progress of hydrogenation and dehydrogenation. Our group and others have looked at other possibilities, such as the 2D/G ratio, the D peak full width at half maximum, and the photoluminescence intensity (see Sec. IV C), to provide more reliable measures of hydrogenation in these highly defected regimes.<sup>7,81</sup>

## IV. PROPERTIES AND APPLICATIONS

Hydrogenated graphene has piqued the interest of a number of research groups because it presents the simplest possible chemical modification of graphene, and yet its properties are generally radically different from those of graphene.

In this section, we examine the electronic, magnetic, optical, and chemical properties of hydrogenated graphene with a focus on possible future applications in each of these areas.

### A. Electronic

Any reaction which disrupts the continuity of the graphene's sp<sup>2</sup> bonding structure will decrease the conductivity of the material. The adatoms act as scattering centers, impeding the flow of electrons through the material.<sup>82,83</sup> Haberer *et al.*<sup>84</sup> used angle-resolved photoelectron spectroscopy and Matis *et al.*<sup>5</sup> used transport measurements to show that the band gap of hydrogenated graphene increases with hydrogen coverage. Son *et al.* confirmed this observation using ultraviolet photoelectron spectroscopy to measure the band gap directly. They found a maximum band gap of 3.9 eV.<sup>85</sup> Our experiments with single-layer Birch-hydrogenated graphene showed that the conductivity of graphene could be completely removed by hydrogenation (sheet resistance >10 GΩ/□) and completely restored via thermal annealing.<sup>13</sup>

In addition to simply scattering the electrons at the site of adsorption, adatoms can also alter the electronic characteristics of the surrounding graphene lattice. For instance, fluorine is strongly electronegative—electron withdrawing—and thus fluorine adatoms tend to p-dope the graphene lattice: the fluorine withdraws electron density from the surrounding carbon atoms, which leads to an increased population of holes in the lattice.<sup>86</sup> We mentioned above that one may expect, based on electronegativity arguments, that the carbon-hydrogen bond in graphene is nonpolar, and hence hydrogen does not strongly dope graphene. This turns out not to be the case. Elias *et al.* initially found a strong p-doping behavior from the hydrogenation [Fig. 8(a)].<sup>12</sup> However, Matis *et al.* later found that this p-doping effect came from adsorbed water molecules and that hydrogen by itself actually n-dopes the graphene, once the sample is assiduously dried [Fig. 8(b)].<sup>5</sup> Our group came to similar conclusions as Matis *et al.* about the doping effect of hydrogen.<sup>13</sup>

Hydrogenated graphene also plays a role as a testbed for examining electronic quantum localization effects. Matis *et al.* observe a low-temperature giant negative magnetoresistance in plasma-hydrogenated graphene at a perpendicular magnetic field of 2.5 T, due to the suppression of defect-mediated localization effects.<sup>87</sup> In addition, the same paper reports a transition from strong localization at low carrier densities ( $n_e < 2.6 \times 10^{11} \text{ cm}^{-2}$ ) to weak localization at higher carrier densities, while Jayasingha *et al.* report a transition from weak to strong localization with increasing hydrogen concentration.<sup>88</sup> Guillemette *et al.* observed an insulator-to-quantum Hall transition in graphene that had been hydrogenated via thermal cracking.<sup>89</sup>

### B. Magnetic

Mathematically, graphene is a bipartite lattice with a half-filled band. Equivalently, this simply means that the unit cell of graphene contains two carbon atoms (which define

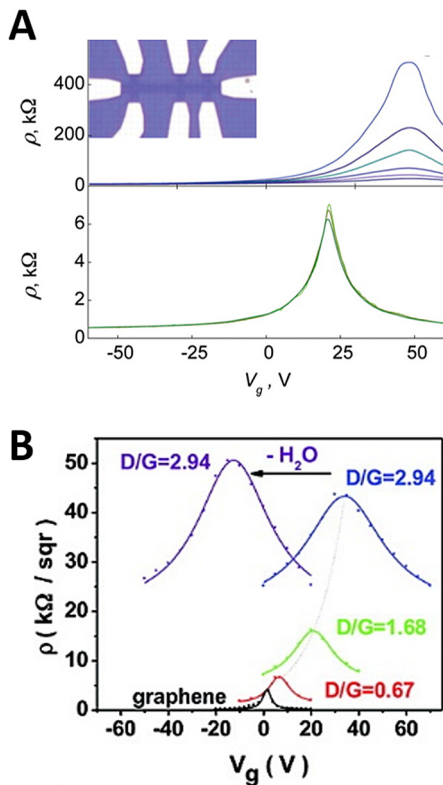


Fig. 8. (a) p-type doping behavior observed in electronic transport measurements of hydrogenated graphene from Elias *et al.* Adapted from Ref. 12 with permission from AAAS. (b) Matis *et al.* showed that adsorbed water was responsible for the p-type doping effect. Adapted from Ref. 5 with permission from the American Chemical Society. Dry hydrogenated graphene is actually n-doped.

sublattices A and B) and each carbon atom contributes one electron to the valence band. Lieb's theorem<sup>90</sup> on this type of system ensures that the total spin of the system is proportional to  $S = \frac{1}{2}|N_A - N_B|$ , the difference between the number of valence electrons coming from the A sublattice and the number of electrons from the B sublattice. In an infinite graphene sheet,  $N_A = N_B$ , so the total spin is zero. However, vacancies, edges, and  $sp^3$  adatom sites all represent removal of those sites' electrons from the valence band of graphene. Thus, if there are more A sublattice vacancies than B sublattice vacancies, the system will theoretically have a nonzero net spin angular momentum and will exhibit magnetic properties. Hydrogenated graphene therefore has the potential to exhibit some interesting magnetic properties.

Real life—also known as the experimental situation—is, as always, more complicated. Lieb's theorem only strictly applies in the case of a bipartite lattice. As such, topological defects in the graphene which scramble the two sublattices (grain boundaries, Stone-Wales defects, etc.) violate this condition. Even in a perfect crystal, Lieb's theorem only tells us that the lattice has a nonzero population of unpaired electrons. It says nothing about whether those electrons are coupled such that the material is ferromagnetic, antiferromagnetic, or paramagnetic. Theorists have attempted to tackle the issue of exchange coupling, with a range of predictions.<sup>91–95</sup> Ultimately, these predictions can either be validated or rendered moot only by

experimental measurement; however, the hydrogenated graphene obtained by existing synthetic methods is noncrystalline. Thus, until a method is discovered for obtaining crystalline hydrogenated graphene, theoretical predictions of this type will have only limited value.

As for the empirical proof itself, a number of groups have presented evidence for a variety of magnetic properties on various forms of hydrogenated graphene. Using superconducting quantum interference device measurements, Xie *et al.*<sup>96</sup> and Eng *et al.*<sup>39</sup> [Fig. 9(g)] found evidence of room-temperature ferromagnetism in hydrogenated epitaxial graphene on SiC and hydrogenated graphene oxide, respectively. Our group found MFM evidence for room-temperature ferromagnetism in single-layer, partially hydrogenated graphene resulting from the Birch reduction [Figs. 9(e) and 9(f)].<sup>48</sup>

One of the most illuminating studies of graphene magnetism was performed by Gonzalez-Herrero *et al.*, who used STM in comparison with theoretical calculations of the local density of states to measure magnetic moments induced by individual hydrogen atoms on graphene.<sup>71</sup> Their work was a direct corroboration of Lieb's theorem on a graphene lattice. They showed that an imbalance of hydrogen adatoms on the graphene sublattices led to a measurable net magnetic moment, while rearranging the hydrogen atom-by-atom to give equal numbers of hydrogen on each sublattice cancelled the magnetic moment [Figs. 9(a)–9(d)].

As with so many other aspects of graphene science, the substrate plays an active role in the magnetism of hydrogenated graphene. Dev and Reinecke predicted theoretically that substrates such as copper could donate electrons into the lattice of a magnetically active hydrogenated graphene configuration to quench the magnetism.<sup>92</sup> Giesbers *et al.* found evidence of room-temperature ferromagnetism in hydrogenated epitaxial graphene on SiC whose presence relied on the existence of the hydrogenated SiC buffer layer directly under the graphene.<sup>97</sup>

Finally, we point out that our own researchers have incorporated hydrogenated graphene into spintronic devices. The hydrogenated graphene serves as the tunnel barrier for spin injection into the graphene carrier channel of a nonlocal spin valve. The tunnel barrier is necessary to overcome the conductivity mismatch problem, and using hydrogenated graphene, it is possible to achieve significant levels of spin polarization.<sup>98,99</sup> This result represents progress toward building practical graphene-based low-power spintronic devices.

### C. Optical

A striking early theoretical result predicted that graphene would have an optical absorption of  $\pi\alpha$  (roughly 2.3%), where  $\alpha$  is the fine structure constant ( $\sim 1/137$ ).<sup>101,102</sup> While this result is idealized, graphene does boast a largely featureless absorption spectrum across a broad range of visible and infrared frequencies where it absorbs roughly 2% of all photons.<sup>103</sup> The broadband absorption of pristine graphene arises from the fact that single-layer graphene's density of states is almost exactly a linear function of photon frequency around the Fermi level.<sup>102</sup> As we have discussed previously,

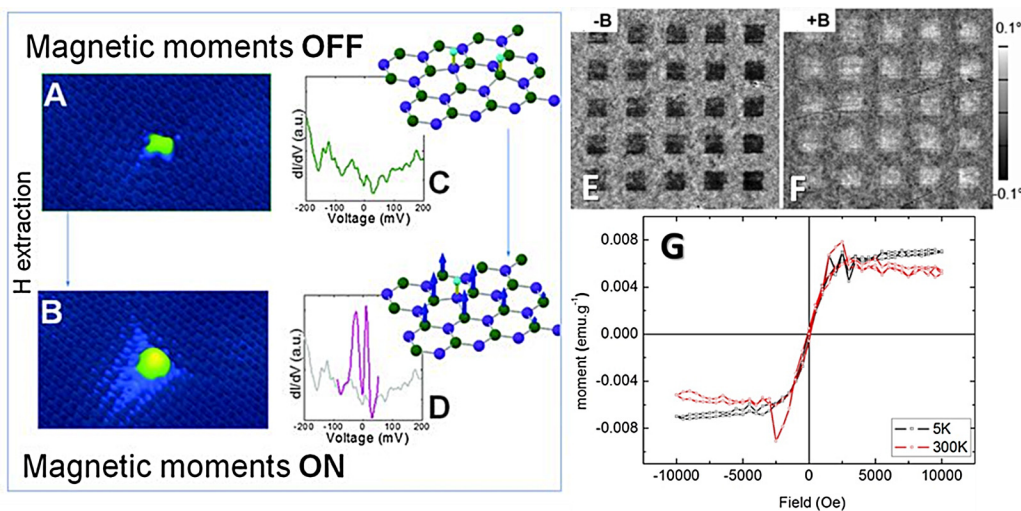


FIG. 9. (a)–(d) Scanning tunneling spectroscopy showing magnetic moments of individual hydrogen atoms on graphene. (a) and (c) are the image and local density of states for two hydrogen atoms on different sublattices. (b) and (d) are the image and local density of states for two hydrogen atoms on the same sublattice. (e) and (f) Magnetic force microscopy images for partially hydrogenated graphene patterned with an electron beam. The images in (e) and (f) were taken with magnetic tips of opposite polarity. (g) Magnetization measurements of highly hydrogenated graphene, showing small hysteresis characteristic of ferromagnetism. (a)–(d) adapted from Ref. 71 with permission from AAAS. (e) and (f) adapted from Ref. 48 with permission from Wiley. (g) Reprinted from Ref. 39 with permission from the American Chemical Society.

however, adding hydrogen to the lattice opens up a band gap in graphene and therefore disturbs the simple functional form found in its density of states. Indeed, theoretical and UV-visible spectroscopic results have pointed to hydrogenated graphene having a tunable band gap, with very heavily hydrogenated material having an optical band gap of around 4 eV [Figs. 10(a) and 10(d)].<sup>5,85,94,95,100</sup> These observations indicate that there should be essentially no absorption of photons less than this threshold energy.

Highly hydrogenated graphene shows depressed levels of light absorption below this band gap. However, one interesting optical property of hydrogenated graphene is its photoluminescence [Fig. 10(c)].<sup>29</sup> Other highly functionalized graphene species, including graphene oxide<sup>104–106</sup> and graphene fluoride,<sup>107</sup> exhibit these photoluminescent properties as well. This phenomenon arises from the fact that, as adatoms populate the graphene lattice stochastically, electronically unconnected conjugated polycyclic regions are formed; these areas demonstrate a broad range of absorption profiles and strongly fluorescent emission properties.<sup>30</sup> These fluorescent regions are functionally equivalent to carbon nanodots. Thus, highly hydrogenated graphene has been considered for similar applications as quantum dots: namely, their white light fluorescence, optoelectronic features, and imaging capabilities.<sup>108</sup>

#### D. Chemical

The most prominent feature of the chemistry of hydrogenated graphene is its reversibility. This feature was noted by Elias *et al.* who showed that graphene could be obtained from the hydrogenated species by heating at 450 °C under argon for 24 h.<sup>12</sup> Later, our group showed that graphene could be restored even from very heavily hydrogenated, completely insulating, graphene with simple heating at

300 °C under argon for 12 h.<sup>13</sup> In fact, applied heating is not necessary for dehydrogenation. Geim and Grigorieva observed that “Graphane (fully hydrogenated graphene) gradually loses its hydrogen and is unlikely to be useful for making heterostructures.”<sup>8</sup> Our group also quantified the chemical, thermal, and ambient dehydrogenation of Birch-hydrogenated single-layer graphene.<sup>6,7</sup>

An important finding with regard to the reversibility of graphene hydrogenation is that single-layer graphene is far easier to dehydrogenate than multilayer graphene.<sup>7,19</sup> This effect is presumably due to the extra kinetic barrier required to unbind and deintercalate hydrogen atoms from the interstitial spaces between graphene layers in multilayer graphene, essentially the reverse of the intercalation process observed during hydrogenation of multilayer graphene.<sup>15</sup>

The dependence of hydrogenated graphene’s stability on layer number has important implications for its usability. Proposed applications of hydrogenated graphene generally either require the hydrogen to remain on the graphene (electronic, magnetic, etc. applications) or require the graphene to release the hydrogen (hydrogen storage for hydrogen economy applications). We have already discussed electronic and magnetic applications in Secs. IV A and IV B. The one point that we add here is that, since even two layers of hydrogenated graphene are up to 10 times more stable than a single layer, future work incorporating hydrogenated graphene into 2D electronic devices might be well advised to consider using few-layer hydrogenated graphene instead of single-layer material to boost device robustness. Alternatively, as our work has pointed out,<sup>7</sup> a single layer of pristine graphene underneath hydrogenated graphene is also adequate to preserve hydrogen functionality well beyond what is observed for the single-layer hydrogenated graphene by itself.

Hydrogenated graphene and graphite are attractive for hydrogen storage for a number of reasons. First, the material

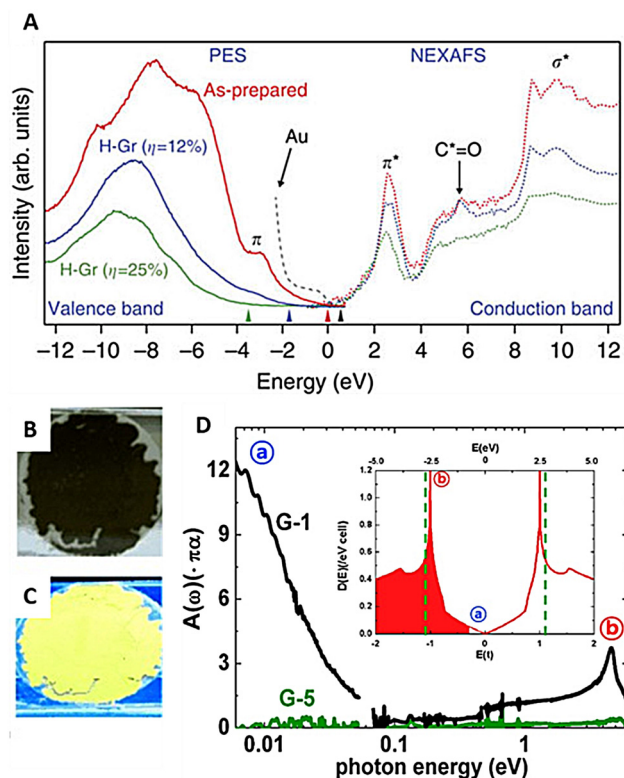


FIG. 10. (a) Ultraviolet photoelectron spectroscopy (PES) and Near-edge x-ray absorption fine structure (NEXAFS) spectroscopy of hydrogenated graphene, giving a direct measure of the optical band gap. Adapted from Ref. 85 under Creative Commons license. (b) and (c) Birch-hydrogenated bulk graphite under visible (b) and UV (c) light, showing intense UV fluorescence. Adapted from Ref. 29 with permission from Wiley. (d) Far-IR to UV spectroscopy of hydrogenated graphene, showing the relatively featureless spectrum in the visible range. Adapted from Ref. 100 with permission from Elsevier.

is lightweight, similar to other solid state hydrogen storage systems such as lithium and boron hydrides. Second, unlike lithium and boron hydrides, hydrogenated graphene is far less toxic and chemically reactive, making it a more attractive target for use in consumer products such as hydrogen cars.<sup>100</sup> Finally, hydrogenated graphene theoretically has an enormous potential for hydrogen storage. Fully hydrogenated graphene is theoretically 7.7% hydrogen by weight. This exceeds the target system of the U.S. Department of Energy, which aims for 5.5% H<sub>2</sub> storage by weight by the year 2020.<sup>109</sup> Using the Birch reduction on graphite oxide, Subrahmanyam *et al.* reported completely thermally reversible hydrogen storage of up to 5% by weight.<sup>47</sup> By replacing liquid ammonia with ethylenediamine and running the Birch reaction at room temperature, Sarkar *et al.* reported a remarkable hydrogen content of 14.67% by weight, as measured by thermogravimetric analysis.<sup>43</sup> One notes that this vastly exceeds the theoretical hydrogen content of fully hydrogenated graphene. Thus, if this result is corroborated, it would show that a significant percentage of this material's hydrogen content is physisorbed, not chemisorbed, hydrogen. Physisorbed hydrogen is easier to put to use than chemisorbed hydrogen, but it is also less stable and more difficult to retain.

Another remarkable and unexpected feature of hydrogenated graphene is that hydrogen adatoms activate graphene toward further functionalization, similar to halogen or oxygen functionalities.<sup>6,110</sup> This is striking because C-H bonds in traditional organic chemistry are basically unreactive—indeed, an entire branch of organic chemistry specifically devoted to C-H activation has developed in the past few decades. These approaches generally involve using some catalyst to polarize the inherently nonpolar C-H bond and thereby activate it toward substitution. However, in the case of hydrogenated graphene, two factors assist in activating the C-H bond. For one, electronic measurements confirm that the hydrogen donates electron density to the graphene lattice, so that strictly speaking, the C-H bond in hydrogenated graphene is somewhat more polar than a comparable bond in a typical organic compound. Second, the lattice distortion caused by the adatom-induced rehybridization of the carbon site from sp<sup>2</sup> to sp<sup>3</sup> weakens the C-H bond, since there is not a significant energy penalty for returning the graphene to planarity.<sup>6</sup> Thus, we observe that high hydrogenation levels activate graphene toward polymer grafting<sup>110</sup> as well as addition of chlorine and certain alkyl radicals.<sup>6</sup>

## E. Other properties

The thermal properties of hydrogenated graphene are surprisingly underreported, especially in light of how extensively the thermal properties of graphene itself have been examined.<sup>111,112</sup> The exceptional thermal transport of graphene has suggested the use of the material in heat dissipation and bolometry. One can imagine similar uses for hydrogenated graphene, with the additional benefit that hydrogenated graphene is insulating—a useful property for heat dissipation in electronics—but with the caveat that the material loses hydrogen at high temperatures (300–500 °C). Theory predicts that thermal transport in hydrogenated graphene is only slightly degraded from that in pristine graphene.<sup>113,114</sup> Hemsworth *et al.* examined the contribution of electron–phonon coupling to heat dissipation at low temperatures in plasma-hydrogenated graphene,<sup>115</sup> but very little other experimental work has been carried out on hydrogenated graphene's thermal properties.

The mechanical properties of hydrogenated graphene are comparable to those of graphene. Elias *et al.* determined a very small change in lattice constant via x-ray diffraction.<sup>12</sup> Molecular dynamics simulations have speculated that patterned hydrogenation could be used to strengthen graphene or fold it into origami shapes for a number of applications.<sup>116,117</sup> These notions have yet to be experimentally demonstrated. In our own work, we have found that the van der Waals force between hydrogenated graphene and its substrate is far weaker than between pristine graphene and a substrate. This allows us to delaminate hydrogenated graphene from its substrate simply by dipping it into water [Figs. 11(a) and 11(b)]. The free-floating hydrogenated graphene can be recovered on an arbitrary substrate. We have used this property to outfit graphene with various chemical and physical functionalities and transfer these properties *in toto* to

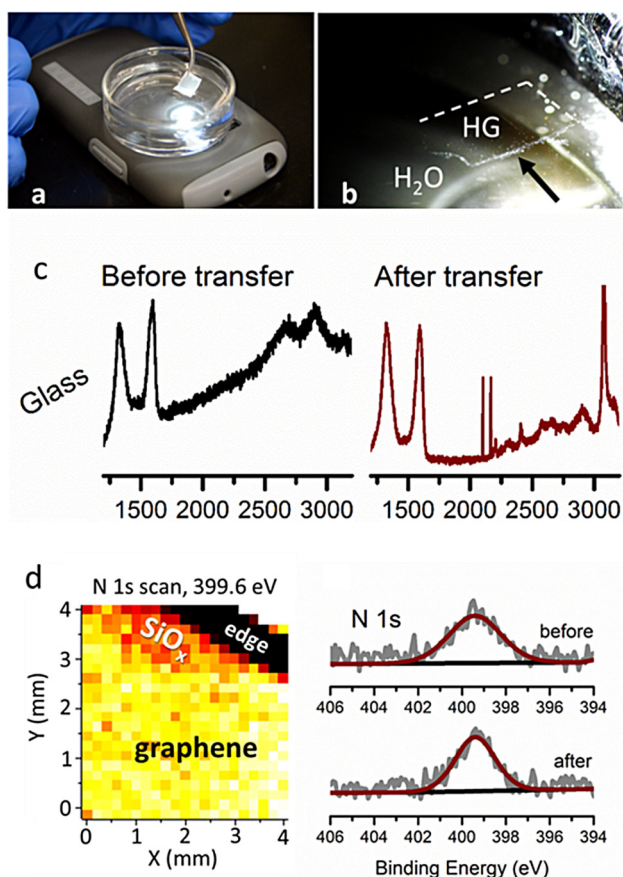


Fig. 11. (a) Delamination of hydrogenated graphene from its substrate in water. (b) Free-floating hydrogenated graphene sheet on the surface of water. (c) Raman spectra of hydrogenated graphene before and after transfer to a glass surface. (d) XPS map and spectrum (N 1s region) of amine-functionalized graphene before and after transfer to SiO<sub>x</sub>. Adapted from Ref. 49 with permission from the American Chemical Society.

arbitrary surfaces [Figs. 11(c) and 11(d)], a significant step toward full control of surface engineering.<sup>7,49</sup> We note that this ability to transfer surface functionality is only possible because hydrogenated graphene is incredibly mechanically strong for a material with subnanometer thickness.

## V. SUMMARY AND OUTLOOK

We have outlined several important aspects of hydrogenated graphene in this review, including practical considerations in its preparation and characterization. In addition, we have pointed to several ongoing areas of active research with respect to applications of hydrogenated graphene. While electronic properties have gotten the most attention, followed by hydrogen storage applications, we are currently witnessing a surge in interest concerning hydrogenated graphene's magnetic and optical properties. In addition, applications such as our own work in surface engineering show that the future of hydrogenated graphene might lie not in any intrinsic property, but rather in the possibilities that the material opens to researchers who are only tangentially attached to the 2D materials community.

Of all the 2D materials discovered thus far, graphene has commanded, and continues to command, by far the most attention. This is in part because graphene was discovered first, but also because of the progress that has been made with regard to chemical functionalization of graphene. By tunably altering the properties of graphene, chemical functionalization effectively broadens graphene from a single 2D material to a large family of 2D materials. As our facility with chemical modification of other 2D materials develops, we can expect to see a similar rise in attention paid to those materials which are most amenable to modification. Hydrogenation represents the simplest possible chemical modification of materials, and as such, receives substantial research effort, both in theoretical and in experimental studies. Indeed, research is already underway on hydrogenation of MoS<sub>2</sub>,<sup>118</sup> silicene,<sup>119</sup> germanene,<sup>120</sup> phosphorene,<sup>121</sup> hexagonal boron nitride,<sup>122</sup> and MXenes,<sup>123</sup> among other species. Thus, hydrogenated graphene will remain a powerful influence in the field of materials science not only for its own sake, but also for the lessons that it will impart to newer and more advanced 2D materials.

## ACKNOWLEDGMENT

K.E.W. is grateful to the NRL Nanoscience Institute Base Program for funding and support.

- <sup>1</sup>K. S. Novoselov, A. K. Geim, S. V. Morozov, D. Jiang, Y. Zhang, S. V. Dubonos, I. V. Grigorieva, and A. A. Firsov, *Science* **306**, 666 (2004).
- <sup>2</sup>V. Georgakilas, M. Otyepka, A. B. Bourlinos, V. Chandra, N. Kim, K. C. Kemp, P. Hobza, R. Zboril, and K. S. Kim, *Chem. Rev.* **112**, 6156 (2012).
- <sup>3</sup>D. R. Dreyer, S. Park, C. W. Bielawski, and R. S. Ruoff, *Chem. Soc. Rev.* **39**, 228 (2010).
- <sup>4</sup>J. O. Sofo, A. S. Chaudhari, and G. D. Barber, *Phys. Rev. B* **75**, 4 (2007).
- <sup>5</sup>B. R. Matis, J. S. Burgess, F. A. Bulat, A. L. Friedman, B. H. Houston, and J. W. Baldwin, *ACS Nano* **6**, 17 (2012).
- <sup>6</sup>K. E. Whitener, W. K. Lee, R. Stine, C. R. Tamanaha, D. A. Kidwell, J. T. Robinson, and P. E. Sheehan, *RSC Adv.* **6**, 93356 (2016).
- <sup>7</sup>K. E. Whitener, J. T. Robinson, and P. E. Sheehan, *Langmuir* **33**, 13749 (2017).
- <sup>8</sup>A. K. Geim and I. V. Grigorieva, *Nature* **499**, 419 (2013).
- <sup>9</sup>M. Pumera and C. H. A. Wong, *Chem. Soc. Rev.* **42**, 5987 (2013).
- <sup>10</sup>C. Zhou, S. H. Chen, J. Z. Lou, J. H. Wang, Q. J. Yang, C. R. Liu, D. P. Huang, and T. H. Zhu, *Nanoscale Res. Lett.* **9**, 26 (2014).
- <sup>11</sup>H. Sahin, O. Leenaerts, S. K. Singh, and F. M. Peeters, *Wires Comput. Mol. Sci.* **5**, 255 (2015).
- <sup>12</sup>D. C. Elias *et al.*, *Science* **323**, 610 (2009).
- <sup>13</sup>K. E. Whitener, Jr., W. K. Lee, P. M. Campbell, J. T. Robinson, and P. E. Sheehan, *Carbon* **72**, 348 (2014).
- <sup>14</sup>U. Bangert, C. T. Pan, R. R. Nair, and M. H. Gass, *Appl. Phys. Lett.* **97**, 253118 (2010).
- <sup>15</sup>X. Zhang *et al.*, *J. Am. Chem. Soc.* **138**, 14980 (2016).
- <sup>16</sup>R. Balog *et al.*, *Nat. Mater.* **9**, 315 (2010).
- <sup>17</sup>A. Felten, D. McManus, C. Rice, L. Nittler, J.-J. Pireaux, and C. Casiraghi, *Appl. Phys. Lett.* **105**, 183104 (2014).
- <sup>18</sup>S. G. Walton, S. C. Hernández, D. R. Boris, B. P. Tz, and G. M. Petrov, *J. Phys. D Appl. Phys.* **50**, 354001 (2017).
- <sup>19</sup>Z. Q. Luo, T. Yu, K. J. Kim, Z. H. Ni, Y. M. You, S. Lim, Z. X. Shen, S. Z. Wang, and J. Y. Lin, *ACS Nano* **3**, 1781 (2009).
- <sup>20</sup>M. Wojtaszek, N. Tombros, A. Caretta, P. H. M. van Loosdrecht, and B. J. van Wees, *J. Appl. Phys.* **110**, 063715 (2011).
- <sup>21</sup>J. D. Jones, W. D. Hoffmann, A. V. Jesseph, C. J. Morris, G. F. Verbeck, and J. M. Perez, *Appl. Phys. Lett.* **97**, 233104 (2010).
- <sup>22</sup>L. Xie, L. Jiao, and H. Dai, *J. Am. Chem. Soc.* **132**, 14751 (2010).

- <sup>23</sup>D. Marinov, *Appl. Phys. Lett.* **108**, 226101 (2016).
- <sup>24</sup>B. Eren, W. Fu, L. Marot, M. Calame, R. Steiner, and E. Meyer, *Appl. Phys. Lett.* **106**, 011904 (2015).
- <sup>25</sup>R. Balog, B. Jørgensen, J. Wells, E. Lægsgaard, P. Hofmann, F. Besenbacher, and L. Hornekær, *J. Am. Chem. Soc.* **131**, 8744 (2009).
- <sup>26</sup>N. P. Guisinger, G. M. Rutter, J. N. Crain, P. N. First, and J. A. Stroscio, *Nano Lett.* **9**, 1462 (2009).
- <sup>27</sup>A. Bostwick, J. L. McChesney, K. V. Emtsev, T. Seyller, K. Horn, S. D. Kevan, and E. Rotenberg, *Phys. Rev. Lett.* **103**, 056404 (2009).
- <sup>28</sup>Z. Q. Yang, Y. Q. Sun, L. B. Alemany, T. N. Narayanan, and W. E. Billups, *J. Am. Chem. Soc.* **134**, 18689 (2012).
- <sup>29</sup>R. A. Schafer, J. M. Englert, P. Wehrfritz, W. Bauer, F. Hauke, T. Seyller, and A. Hirsch, *Angew. Chem. Int. Ed.* **52**, 754 (2013).
- <sup>30</sup>V. Strauss, R. A. Schäfer, F. Hauke, A. Hirsch, and D. M. Guldi, *J. Am. Chem. Soc.* **137**, 13079 (2015).
- <sup>31</sup>Y. Yang, Y. Li, Z. Huang, and X. Huang, *Carbon* **107**, 154 (2016).
- <sup>32</sup>J. M. Englert, K. C. Knirsch, C. Dotzer, B. Butz, F. Hauke, E. Spiecker, and A. Hirsch, *Chem. Commun.* **48**, 5025 (2012).
- <sup>33</sup>A. Hirsch, J. M. Englert, and F. Hauke, *Acc. Chem. Res.* **46**, 87 (2013).
- <sup>34</sup>K. M. Daniels, B. K. Daas, N. Srivastava, C. Williams, R. M. Feenstra, T. S. Sudarshan, and M. V. S. Chandrashekar, *J. Appl. Phys.* **111**, 7 (2012).
- <sup>35</sup>M. Zhao, X.-Y. Guo, O. Ambacher, C. E. Nebel, and R. Hoffmann, *Carbon* **83**, 128 (2015).
- <sup>36</sup>C.-Y. Su, A.-Y. Lu, Y. Xu, F.-R. Chen, A. N. Khlobystov, and L.-J. Li, *ACS Nano* **5**, 2332 (2011).
- <sup>37</sup>Y. L. Zhong and T. M. Swager, *J. Am. Chem. Soc.* **134**, 17896 (2012).
- <sup>38</sup>A. Dey, A. Chroneos, N. S. J. Braithwaite, R. P. Gandhiraman, and S. Krishnamurthy, *Appl. Phys. Rev.* **3**, 021301 (2016).
- <sup>39</sup>A. Y. S. Eng, H. L. Poh, F. Sanek, M. Marysko, S. Matejkova, Z. Sofer, and M. Pumera, *ACS Nano* **7**, 5930 (2013).
- <sup>40</sup>L. Zheng, Z. Li, S. Bourdo, F. Watanabe, C. C. Ryerson, and A. S. Biris, *Chem. Commun.* **47**, 1213 (2011).
- <sup>41</sup>A. J. Birch, *J. Chem. Soc. (Resumed)* 430 (1944).
- <sup>42</sup>A. Y. S. Eng, Z. Sofer, Š Huber, D. Bouša, M. Maryško, and M. Pumera, *Chem. Eur. J.* **21**, 16828 (2015).
- <sup>43</sup>A. K. Sarkar, S. Saha, S. Ganguly, D. Banerjee, and K. Kargupta, *Int. J. Energy Res.* **38**, 1889 (2014).
- <sup>44</sup>R. A. Schäfer, D. Dasler, U. Mundloch, F. Hauke, and A. Hirsch, *J. Am. Chem. Soc.* **138**, 1647 (2016).
- <sup>45</sup>X. Zhang, K. Goossens, W. Li, X. Chen, X. Chen, M. Saxena, S. H. Lee, C. W. Bielawski, and R. S. Ruoff, *Carbon* **121**, 309 (2017).
- <sup>46</sup>I. Papadakis *et al.*, *J. Phys. Chem. C* **121**, 22567 (2017).
- <sup>47</sup>K. S. Subrahmanyam, P. Kumar, U. Maitra, A. Govindaraj, K. Hembram, U. V. Waghmare, and C. N. R. Rao, *Proc. Natl. Acad. Sci. U.S.A.* **108**, 2674 (2011).
- <sup>48</sup>W.-K. Lee, K. E. Whitener, J. T. Robinson, and P. E. Sheehan, *Adv. Mater.* **27**, 1774 (2015).
- <sup>49</sup>K. E. Whitener, W. K. Lee, N. D. Bassim, R. M. Stroud, J. T. Robinson, and P. E. Sheehan, *Nano Lett.* **16**, 1455 (2016).
- <sup>50</sup>J. Wang, K. K. Manga, Q. Bao, and K. P. Loh, *J. Am. Chem. Soc.* **133**, 8888 (2011).
- <sup>51</sup>Z. Sofer, O. Jankovsky, A. Libanska, P. Simek, M. Novacek, D. Sedmidubsky, A. Mackova, R. Miksova, and M. Pumera, *Nanoscale* **7**, 10535 (2015).
- <sup>52</sup>Z. Sofer, O. Jankovsky, P. Simek, L. Soferova, D. Sedmidubsky, and M. Pumera, *Nanoscale* **6**, 2153 (2014).
- <sup>53</sup>S. Ryu, M. Y. Han, J. Maultzsch, T. F. Heinz, P. Kim, M. L. Steigerwald, and L. E. Brus, *Nano Lett.* **8**, 4597 (2008).
- <sup>54</sup>W. Chen, Z. Zhu, S. Li, C. Chen, and L. Yan, *Nanoscale* **4**, 2124 (2012).
- <sup>55</sup>J. Kintigh, B. Diaconescu, Y. Echegoyen, A. Busnaina, K. Pohl, and G. P. Miller, *Diam. Relat. Mater.* **66**, 107 (2016).
- <sup>56</sup>S. J. Tjung, S. M. Hollen, G. A. Gambrel, N. M. Santagata, E. Johnston-Halperin, and J. A. Gupta, *Carbon* **124**, 97 (2017).
- <sup>57</sup>I.-S. Byun *et al.*, *ACS Nano* **5**, 6417 (2011).
- <sup>58</sup>Q. H. Wang *et al.*, *Nat. Chem.* **4**, 724 (2012).
- <sup>59</sup>R. Stine, W.-K. Lee, K. E. Whitener, J. T. Robinson, and P. E. Sheehan, *Nano Lett.* **13**, 4311 (2013).
- <sup>60</sup>S. Son, C. Holroyd, J. Clough, A. Horn, S. P. K. Koehler, and C. Casiraghi, *Appl. Phys. Lett.* **109**, 243103 (2016).
- <sup>61</sup>C. Lin *et al.*, *Nano Lett.* **15**, 903 (2015).
- <sup>62</sup>M. L. Ng, R. Balog, L. Hornekær, A. B. Preobrajenski, N. A. Vinogradov, N. Mårtensson, and K. Schulte, *J. Phys. Chem. C* **114**, 18559 (2010).
- <sup>63</sup>D. Solenov, C. Junkermeier, T. L. Reinecke, and K. A. Velizhanin, *Phys. Rev. Lett.* **111**, 115502 (2013).
- <sup>64</sup>S. Pekker, J. P. Salvetat, E. Jakab, J. M. Bonard, and L. Forro, *J. Phys. Chem. B* **105**, 7938 (2001).
- <sup>65</sup>C. Cavallari *et al.*, *J. Phys. Conf. Ser.* **554**, 012009 (2014).
- <sup>66</sup>E. F. Sheka and I. Natkaniec, *Rev. Adv. Mater. Sci.* **49**, 1 (2017).
- <sup>67</sup>V. Mazanek, O. Jankovsky, J. Luxa, D. Sedmidubsky, Z. Janousek, F. Sembera, M. Mikulics, and Z. Sofer, *Nanoscale* **7**, 13646 (2015).
- <sup>68</sup>M. Currie, J. D. Caldwell, F. J. Bezares, J. Robinson, T. Anderson, H. Chun, and M. Tadjer, *Appl. Phys. Lett.* **99**, 211909 (2011).
- <sup>69</sup>S. F. Spanò, G. Isgrò, P. Russo, M. E. Fragalà, and G. Compagnini, *Appl. Phys. A* **117**, 19 (2014).
- <sup>70</sup>H. Zhang, Y. Miyamoto, and A. Rubio, *Phys. Rev. B* **85**, 201409 (2012).
- <sup>71</sup>H. Gonzalez-Herrero *et al.*, *Science* **352**, 437 (2016).
- <sup>72</sup>J. R. Felts, A. J. Oyer, S. C. Hernández, K. E. Whitener, Jr., J. T. Robinson, S. G. Walton and P. E. Sheehan, *Nat. Commun.* **6**, 6467 (2015).
- <sup>73</sup>U. Bangert, M. Gass, R. Zan, and C. T. Pan, *Physics and Applications of Graphene - Experiments*, edited by S. Mikhailov (InTechOpen, London, 2011), Chap. 15, pp. 377–408.
- <sup>74</sup>C. Riedl, C. Coletti, T. Iwasaki, A. A. Zakharov, and U. Starke, *Phys. Rev. Lett.* **103**, 246804 (2009).
- <sup>75</sup>C. Cavallari, D. Pontiroli, M. Jimenez-Ruiz, M. Johnson, M. Aramini, M. Gaboardi, S. F. Parker, M. Ricco, and S. Rols, *Phys. Chem. Chem. Phys.* **18**, 24820 (2016).
- <sup>76</sup>I. Natkaniec, E. F. Sheka, K. Druzbecki, K. Holderna-Natkaniec, S. P. Gubin, E. Y. Buslaeva, and S. V. Tkachev, *J. Phys. Chem. C* **119**, 18650 (2015).
- <sup>77</sup>A. Jorio, M. Dresselhaus, R. Saito, and G. F. Dresselhaus, *Raman Spectroscopy in Graphene Related Systems* (Wiley-VCH, Weinheim, 2011).
- <sup>78</sup>A. C. Ferrari and D. M. Basko, *Nat. Nanotechnol.* **8**, 235 (2013).
- <sup>79</sup>A. C. Ferrari *et al.*, *Phys. Rev. Lett.* **97**, 4 (2006).
- <sup>80</sup>M. M. Lucchese, F. Stavale, E. H. M. Ferreira, C. Vilani, M. V. O. Moutinho, R. B. Capaz, C. A. Achete, and A. Jorio, *Carbon* **48**, 1592 (2010).
- <sup>81</sup>E. H. Martins Ferreira, M. V. O. Moutinho, F. Stavale, M. M. Lucchese, R. B. Capaz, C. A. Achete, and A. Jorio, *Phys. Rev. B* **82**, 125429 (2010).
- <sup>82</sup>T. O. Wehling, M. I. Katsnelson, and A. I. Lichtenstein, *Chem. Phys. Lett.* **476**, 125 (2009).
- <sup>83</sup>J. Katoch, J. H. Chen, R. Tsuchikawa, C. W. Smith, E. R. Mucciolo, and M. Ishigami, *Phys. Rev. B* **82**, 081417 (2010).
- <sup>84</sup>D. Haberer *et al.*, *Nano Lett.* **10**, 3360 (2010).
- <sup>85</sup>J. Son, S. Lee, S. J. Kim, B. C. Park, H. K. Lee, S. Kim, J. H. Kim, B. H. Hong, and J. Hong, *Nat. Commun.* **7**, 13261 (2016).
- <sup>86</sup>J. T. Robinson *et al.*, *Nano Lett.* **10**, 3001 (2010).
- <sup>87</sup>B. R. Matis, F. A. Bulat, A. L. Friedman, B. H. Houston, and J. W. Baldwin, *Phys. Rev. B* **85**, 105437 (2012).
- <sup>88</sup>R. Jayasingha, A. Sherehiy, S.-Y. Wu, and G. U. Sumanasekera, *Nano Lett.* **13**, 5098 (2013).
- <sup>89</sup>J. Guilletette *et al.*, *Phys. Rev. Lett.* **110**, 176801 (2013).
- <sup>90</sup>E. H. Lieb, *Phys. Rev. Lett.* **62**, 1201 (1989).
- <sup>91</sup>D. Soriano, F. Muñoz-Rojas, J. Fernández-Rossier, and J. J. Palacios, *Phys. Rev. B* **81**, 165409 (2010).
- <sup>92</sup>P. Dev and T. L. Reinecke, *Phys. Rev. B* **89**, 035404 (2014).
- <sup>93</sup>S. Hemmatiyani, M. Polini, A. Abanov, A. H. MacDonald, and J. Sinova, *Phys. Rev. B* **90**, 035433 (2014).
- <sup>94</sup>J. Zhou, Q. Wang, Q. Sun, X. S. Chen, Y. Kawazoe, and P. Jena, *Nano Lett.* **9**, 3867 (2009).
- <sup>95</sup>L. Feng and W. X. Zhang, *AIP Adv.* **2**, 042138 (2012).
- <sup>96</sup>L. Xie *et al.*, *Appl. Phys. Lett.* **98**, 193113 (2011).
- <sup>97</sup>A. J. M. Giesbers, K. Uhlirva, M. Konecny, E. C. Peters, M. Burghard, J. Aarts, and C. F. J. Flipse, *Phys. Rev. Lett.* **111**, 166101 (2013).
- <sup>98</sup>A. L. Friedman, O. M. J. van 't Erve, J. T. Robinson, K. E. Whitener, and B. T. Jonker, *ACS Nano* **9**, 6747 (2015).
- <sup>99</sup>A. L. Friedman, O. M. J. van't Erve, J. T. Robinson, K. E. Whitener, and B. T. Jonker, *AIP Adv.* **6**, 056301 (2016).
- <sup>100</sup>C. Lee, N. Leconte, J. Kim, D. Cho, I.-W. Lyo, and E. J. Choi, *Carbon* **103**, 109 (2016).

- <sup>101</sup>R. R. Nair, P. Blake, A. N. Grigorenko, K. S. Novoselov, T. J. Booth, T. Stauber, N. M. R. Peres, and A. K. Geim, *Science* **320**, 1308 (2008).
- <sup>102</sup>A. B. Kuzmenko, E. van Heumen, F. Carbone, and D. van der Marel, *Phys. Rev. Lett.* **100**, 117401 (2008).
- <sup>103</sup>K. F. Mak, L. Ju, F. Wang, and T. F. Heinz, *Solid State Commun.* **152**, 1341 (2012).
- <sup>104</sup>G. Eda, Y.-Y. Lin, C. Mattevi, H. Yamaguchi, H.-A. Chen, I. S. Chen, C.-W. Chen, and M. Chhowalla, *Adv. Mater.* **22**, 505 (2010).
- <sup>105</sup>T. V. Cuong, V. H. Pham, Q. T. Tran, S. H. Hahn, J. S. Chung, E. W. Shin, and E. J. Kim, *Mater. Lett.* **64**, 399 (2010).
- <sup>106</sup>Z. Luo, P. M. Vora, E. J. Mele, A. T. C. Johnson, and J. M. Kikkawa, *Appl. Phys. Lett.* **94**, 111909 (2009).
- <sup>107</sup>K.-J. Jeon *et al.*, *ACS Nano* **5**, 1042 (2011).
- <sup>108</sup>H. Li, Z. Kang, Y. Liu, and S.-T. Lee, *J. Mater. Chem.* **22**, 24230 (2012).
- <sup>109</sup>Fuel Cell Technologies Office, edited by U.S. Dept. of Energy (Washington, DC, 2012).
- <sup>110</sup>M. Seifert, A. H. R. Koch, F. Deubel, T. Simmet, L. H. Hess, M. Stutzmann, R. Jordan, J. A. Garrido, and I. D. Sharp, *Chem. Mater.* **25**, 466 (2013).
- <sup>111</sup>J. H. Seol *et al.*, *Science* **328**, 213 (2010).
- <sup>112</sup>Y. M. Zuev, W. Chang, and P. Kim, *Phys. Rev. Lett.* **102**, 096807 (2009).
- <sup>113</sup>A. H. Reshak, *J. Appl. Phys.* **117**, 225104 (2015).
- <sup>114</sup>G. Barbarino, C. Melis, and L. Colombo, *Carbon* **80**, 167 (2014).
- <sup>115</sup>N. Hemsworth, F. Mahvash, P. L. Lévesque, M. Sijaj, R. Martel, and T. Szkopek, *Phys. Rev. B* **92**, 241411 (2015).
- <sup>116</sup>S. Zhu and T. Li, *ACS Nano* **8**, 2864 (2014).
- <sup>117</sup>Y. Li, D. Datta, S. Li, Z. Li, and V. B. Shenoy, *Comput. Mater. Sci.* **93**, 68 (2014).
- <sup>118</sup>S. W. Han *et al.*, *Phys. Rev. Lett.* **110**, 247201 (2013).
- <sup>119</sup>J. Qiu, H. Fu, Y. Xu, Q. Zhou, S. Meng, H. Li, L. Chen, and K. Wu, *ACS Nano* **9**, 11192 (2015).
- <sup>120</sup>M. Houssa, E. Scalise, K. Sankaran, G. Pourtois, V. V. Afanas'ev, and A. Stesmans, *Appl. Phys. Lett.* **98**, 223107 (2011).
- <sup>121</sup>D. W. Boukhvalov, A. N. Rudenko, D. A. Prishchenko, V. G. Mazurenko, and M. I. Katsnelson, *Phys. Chem. Chem. Phys.* **17**, 15209 (2015).
- <sup>122</sup>F. Späth, J. Gebhardt, F. Düll, U. Bauer, P. Bachmann, C. Gleichweit, A. Göring, H. P. Steinrück, and C. Papp, *2D Mater.* **4**, 035026 (2017).
- <sup>123</sup>H. Pan, *Sci. Rep.* **6**, 32531 (2016).